Local Bifurcations of Nonlinear Hybrid Systems

Quentin Brandon†, Tetsushi Ueta†, Takuji Kousaka‡, and Danièle Fournier-Prunaret+

†Center for Advanced Information Technology
Faculty of Engineering, Tokushima University
2-1 Minami-Josanjima, Tokushima, 770-8506 JAPAN
‡Dept. of Mechanical and Energy Systems Engineering
Faculty of Engineering, Oita University
700 Dannoharu, Oita, 870-1192 JAPAN
+ INSA-DGEI
135 Avenue de Rangueil, Toulouse, 31077 France
Email: {qbrandon,tetsushi}@is.tokushima-u.ac.jp , takuji@cc.oita-u.ac.jp, daniele.fournier@insa-toulouse.fr

Abstract—As most analysis tools for nonlinear dynamical systems are dedicated to either continuous or discrete models, we propose an analysis method for hybrid systems. Using the Poincaré map, we transform the results of partial analysis over the continuous components into a discrete mapping. We can then apply more conventional methods in order to seek for critical values and obtain bifurcation diagrams in the parameters space. In this paper, we describe this method, discuss different approaches to conduct such analysis, and finally present an application example with a 3-state Alpazur oscillator.

1. Introduction

Hybrid systems are mostly the result of continuous systems that undergo discrete changes. It can take various forms: apparition of frictions in a mechanical system, switch in an electronic circuit. Though the solution function to model those systems usually remains continuous, it presents points of non-derivability where such discrete changes occur. We propose using a relevant Poincaré map in order to adapt more usual methods and conduct the bifurcation analysis. We will also consider the numerical implementation aspects and illustrate it with some results of a modified version of the Alpazur oscillator.

2. Principles

2.1. Modeling the System

Let us consider a system written by a set of differential equations defined by smooth functions piecewisely, i.e., for the state i:

$$\frac{dX}{dt} = f_i(X), \tag{1}$$

where,

$$X(t) = \begin{pmatrix} x_0 \\ \vdots \\ x_{n-1} \end{pmatrix} \in R^n. \tag{2}$$

Within each state there is a solution function such as:

$$X_i(t) = \varphi_i(t, X_{i0}) \quad \text{with} \quad X_i(0) = X_{i0}, \tag{3}$$

where X_{i0} is an arbitrary initial value.
Now, based on the switching rules and the definition of a period of our system, we set the Poincaré map, placing its sections at the switching points. We assume for now that the switching conditions for each state can be expressed as a function of the system variables. e.g., for the state i: $q_i(X) = 0$.
The map is therefore expressed as:

$$\begin{aligned} &\Pi_i = \{X_i \in R^n \mid q_i = 0\} \\ &T_i : \quad \Pi_i \to \Pi_{i+1} \\ &\qquad X_i \mapsto X_{i+1} = X_i(\tau_i) = \varphi_i(\tau_i, X_i(0)). \end{aligned} \tag{4}$$

We are now able to perform a local analysis over each partial orbit delimited by those Poincaré sections. Thus the Poincaré mapping is defined as a differentiable map:

$$T = \prod T_i. \tag{5}$$

We finally apply a projection from R^n to R^{n-1} due to the equation of the final state switch condition $q_{m-1} = 0$:

$$\begin{aligned} p \quad : \quad &\Pi_0 \to \Sigma_0 \\ &X_0 \mapsto U_0, \end{aligned} \tag{6}$$

which we use as a discrete definition of our system.

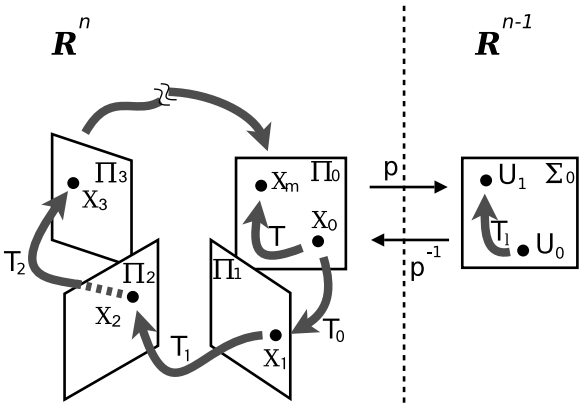

Figure 1: Abstract representation of the Poincaré map

2.2. Analysis approach

In order to compute phase portraits for a given system, we simply integrate the differential equations. The switching conditions previously defined are constantly verified in order to use the variational equations matching the current state. We usually employ a Runge Kutta method due to its performances.
For the computation of fixed points, we integrate the partial derivatives of the differential equations in parallel of the solution:

$$\frac{d}{dt}\frac{\partial \varphi_i}{\partial X_{i-1}} = \frac{\partial f_i}{\partial X}\frac{\partial \varphi_i}{\partial X_{i-1}} \quad \text{where} \quad \frac{\partial \varphi_i}{\partial X_{i-1}}(0) = I. \tag{7}$$

We compute the Jacobian matrix of each local map:

$$\frac{dX_i}{dX_{i-1}} = \frac{\partial \varphi_i}{\partial X_{i-1}} + \frac{dX_i}{dt}\frac{\partial \tau_i}{\partial X_{i-1}}, \tag{8}$$

thus we can express the Poincaré map:

$$\frac{dX_m}{dX_0} = \prod \frac{dX_i}{dX_{i-1}}. \tag{9}$$

We then apply the projection p and obtain the Jacobian:

$$DT_l(U_0) = \frac{dU_m}{dU_0}. \tag{10}$$

For a fixed point we solve:

$$T_l(U_0) = U_m = U_0. \tag{11}$$

We inject the approximation of the tangent to the solution DT_l in the Newton method in order to compute an accurate value of U_0. If our initial value is in the domain of convergence, we converge toward the solution within a few iterations.
Finally, concerning the critical values required to compute bifurcation diagrams, we use the characteristic equation of our system in order to determine an extra equation. Depending on the desired bifurcation diagram, we choose λ, one of the parameters from the diagram space, as an extra degree of freedom to compute a solution of our new equations set:

$$\chi_l(\mu) = \det(DT_l - \mu I_{n-1}) = 0. \tag{12}$$

μ is defined by the bifurcation type. So our new problem can be written:

$$F(U_0, \lambda) = \begin{bmatrix} U_m - U_0 \\ \chi_l(\mu) \end{bmatrix} = 0. \tag{13}$$

Which means we are to compute the following Jacobian matrix:

$$\begin{bmatrix} \dfrac{dU_m}{dU_0} - I_{n-1} & \dfrac{dU_m}{d\lambda} \\ \dfrac{dDT_l}{dU_0} & \dfrac{dDT_l}{d\lambda} \end{bmatrix} \tag{14}$$

The second row of Eq. (13) requires the second derivatives of the solutions of variational equation (7). Computing a number of second derivatives can be done two ways: one based on an analytical approach, consisting in simply deriving once more the first derivative elements; the second one is more numerical since it consists in approaching the tangent by differentiation, performing a multiple integration using Δ shifted input variables. The first approach might appear more elegant but depending on the switching conditions, even the simplest models will involve very elaborated equations at this step. Let us now consider the second alternative: we compute the following elements the same way we did in the fixed point algorithm:

$$\begin{array}{lll} U_m(U_0, \lambda), & U_m(U_0 + \Delta U, \lambda), & U_m(U_0, \lambda + \Delta\lambda), \\ DT_l(U_0, \lambda), & DT_l(U_0 + \Delta U, \lambda), & DT_l(U_0, \lambda + \Delta\lambda). \end{array} \tag{15}$$

We derive the Jacobian matrix elements by differentiation:

$$\begin{aligned} \frac{dU_m}{dU_0} &= \frac{U_m(U_0 + \Delta U, \lambda) - U_m(U_0, \lambda)}{\Delta U} \\ \frac{dU_m}{d\lambda} &= \frac{U_m(U_0, \lambda + \Delta\lambda) - U_m(U_0, \lambda)}{\Delta\lambda} \\ \frac{dDT_l}{dU_0} &= \frac{DT_l(U_0 + \Delta U, \lambda) - DT_l(U_0, \lambda)}{\Delta U} \\ \frac{dDT_l}{d\lambda} &= \frac{DT_l(U_0, \lambda + \Delta\lambda) - DT_l(U_0, \lambda)}{\Delta\lambda}. \end{aligned} \tag{16}$$

The second approach introduces some tricky questions such as how to determine a relevant Δ, but it turns out to be much easier to implement and gives satisfying performances.

3. Three-States Alpazur oscillator

3.1. Model description

In order to illustrate our method with some results, we will now consider the analysis of this slightly modified version of Alpazur oscillator.

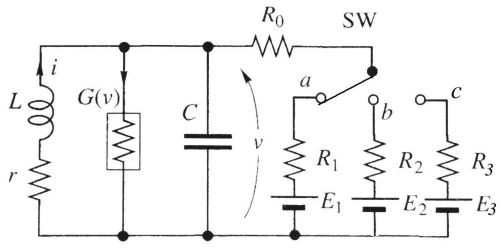

Figure 2: 3-States Alpazur oscillator

The continuous portion of the system is merely a BVP oscillator, while the discrete feature is relying on a switch. The position of the latter represents the current state. By using suitable transformations on the variables, we can extract the following model:
For State 1:

$$\begin{cases} \frac{dx}{dt} = f_0(x, y) = -rx - y \\ \frac{dy}{dt} = g_0(x, y) = x + (1 - A_0)y - \frac{1}{3}y^3 + B_0. \end{cases} \tag{17}$$

For State 2:

$$\begin{cases} \frac{dx}{dt} = f_1(x,y) = -rx - y \\ \frac{dy}{dt} = g_1(x,y) = x + (1 - A_1)y - \frac{1}{3}y^3 + B_1. \end{cases} \tag{18}$$

For State 3:

$$\begin{cases} \frac{dx}{dt} = f_2(x,y) = -rx - y \\ \frac{dy}{dt} = g_2(x,y) = x + (1 - A_2)y - \frac{1}{3}y^3 + B_2. \end{cases} \tag{19}$$

Now for the switching rules:

$$\begin{aligned} q_0 &= y - h \\ q_1 &= y - b \\ q_2 &= y - m, \end{aligned} \tag{20}$$

and the following switching order:

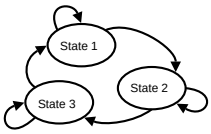

Figure 3: Simple State switching order view

This results in the following type of phase portrait in the multiple State-associated plans view:

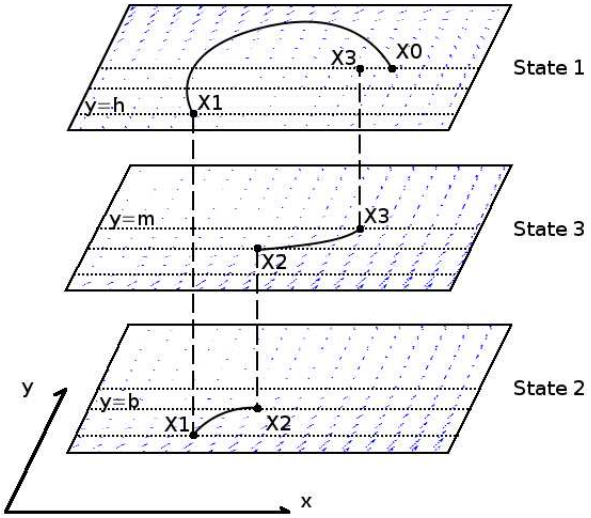

Figure 4: Hysteresis of the switching constraints of Alpazur oscillator

Such model is very convenient because the mapping is strait forward: even within the local maps, y values are fixed thanks to the switching conditions. We can therefore extract the mapped variable $u = x$. We define the map:

$$\begin{array}{lcccl} T_0 & : & \Pi_0 & \to & \Pi_1 \\ & & x_0 & \mapsto & x_1 = \varphi_0(\tau_0, x_1, y_1) \\ & & y_0 & \mapsto & y_1 = \phi_0(\tau_0, x_1, y_1) = h \\ T_1 & : & \Pi_1 & \to & \Pi_2 \\ & & x_1 & \mapsto & x_2 = \varphi_1(\tau_1, x_2, y_2) \\ & & y_1 & \mapsto & y_2 = \phi_1(\tau_1, x_2, y_2) = b \\ T_2 & : & \Pi_2 & \to & \Pi_0 \\ & & x_2 & \mapsto & x_3 = \varphi_2(\tau_2, x_3, y_3) \\ & & y_2 & \mapsto & y_3 = \phi_2(\tau_2, x_3, y_3) = m \\ T = T_0 \circ T_1 \circ T_2 & : & \Pi_0 & \to & \Pi_0 \\ & & x_0 & \mapsto & x_3 = \varphi(\tau, x_3). \end{array} \tag{21}$$

3.2. Fixed points

As previously exposed, the problem of Fixed points is as follows:

$$x_3 - x_0 = 0. \tag{22}$$

In order to compute the appropriate correction, we need to compute:

$$DT_l = \frac{dx_3}{dx_0} = \frac{dx_3}{dx_2}\frac{dx_2}{dx_1}\frac{dx_1}{dx_0}. \tag{23}$$

For each State i we compute:

$$\begin{aligned} \frac{dx_i}{dx_{i-1}} &= \frac{\partial \varphi_i}{\partial x_{i-1}} + f_i(x_i, y_i)\frac{\partial \tau_i}{\partial x_{i-1}} \\ \frac{\partial \tau_i}{\partial x_{i-1}} &= \frac{-\frac{\partial \phi_i}{\partial x_{i-1}}}{g_i(x_i, y_i)}, \end{aligned} \tag{24}$$

where we numerically integrate the required elements:

$$\begin{aligned} &\frac{d}{dt}\begin{bmatrix} x_i \\ y_i \end{bmatrix} = \begin{bmatrix} f_i(x,y) \\ g_i(x,y) \end{bmatrix} \quad \begin{array}{l} \text{State 1: from } x_0 \\ \text{State 2: from } x_1 \\ \text{State 3: from } x_2 \end{array} \\ &\frac{d}{dt}\begin{bmatrix} \frac{\partial \varphi_i}{\partial x_{i-1}} \\ \frac{\partial \phi_i}{\partial x_{i-1}} \end{bmatrix} = \begin{bmatrix} \frac{\partial f_i}{\partial x} & \frac{\partial f_i}{\partial y} \\ \frac{\partial g_i}{\partial x} & \frac{\partial g_i}{\partial y} \end{bmatrix}\begin{bmatrix} \frac{\partial \varphi_i}{\partial x_{i-1}} \\ \frac{\partial \phi_i}{\partial x_{i-1}} \end{bmatrix} \\ &\text{where } \begin{bmatrix} \frac{\partial \varphi_i}{\partial x_{i-1}} \\ \frac{\partial \phi_i}{\partial x_{i-1}} \end{bmatrix}(0) = \begin{bmatrix} 1 \\ 0 \end{bmatrix}. \end{aligned} \tag{25}$$

We now use the Newton method to compute the correction to be applied:

$$x_0' = x_0 - \frac{x_3 - x_0}{\frac{dx_3}{dx_0}}. \tag{26}$$

We obtain fixed points such as in the following phase portrait:

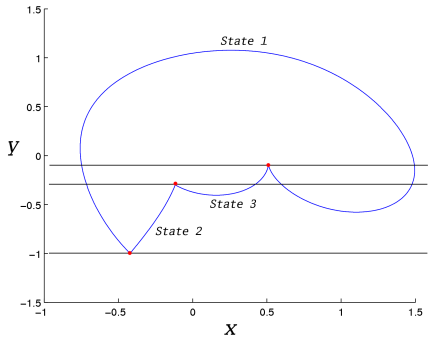

Figure 5: Phase portrait of a single period at the critical value (period-doubling bifurcation)

3.3. Critical values

In this case the characteristic equation is fairly simple:

$$\chi(\mu) = \det(DT_l - \mu) = 0, \tag{27}$$

hence the Jacobian matrix:

$$\begin{bmatrix} \frac{\partial x_3}{\partial x_0} - 1 & \frac{\partial x_3}{\partial \lambda} \\ \frac{\partial DT_l}{\partial x_0} & \frac{\partial DT_l}{\partial \lambda} \end{bmatrix} \tag{28}$$

We compute its elements:

$$\begin{aligned}
\frac{dx_3}{dx_0} &= \frac{x_3(x_0+\Delta x,\lambda)-x_3(x_0,\lambda)}{\Delta x} \\
\frac{dx_3}{d\lambda} &= \frac{x_3(x_0,\lambda+\Delta\lambda)-x_3(x_0,\lambda)}{\Delta\lambda} \\
\frac{dDT_l}{dx_0} &= \frac{\frac{\partial x_3}{\partial x_0}(x_0+\Delta x,\lambda)-\frac{\partial x_3}{\partial x_0}(x_0,\lambda)}{\Delta x} \\
\frac{dDT_l}{d\lambda} &= \frac{\frac{\partial x_3}{\partial x_0}(x_0,\lambda+\Delta\lambda)-\frac{\partial x_3}{\partial x_0}(x_0,\lambda)}{\Delta\lambda}.
\end{aligned} \tag{29}$$

Through combination with conventional methods, we obtain the following results:

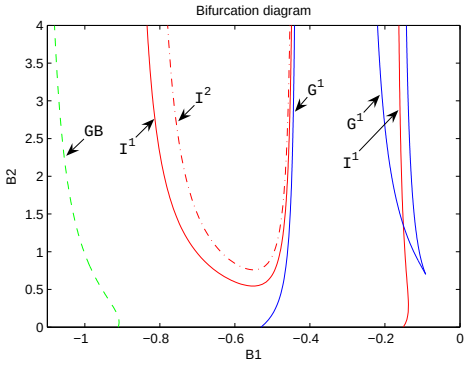

Figure 6: Bif. diagram of the 3-state Alpazur oscillator

In the B_1 / B_2 parameter space, and for the following parameter values:

$r = 0.1$ $A_1 = 0.2$ $A_2 = 2.0$ $A_3 = 0.8$
$B_3 = -0.1$ $m = -0.1$ $b = -0.3$ $h = -1.0$

I stands for *period doubling* bifurcation ($\mu = -1$), while G stands for *tangent* bifurcation ($\mu = 1$), and finally GB stands for *global* bifurcation (here *collision* bifurcation). We illustrate these results with some phase portraits:

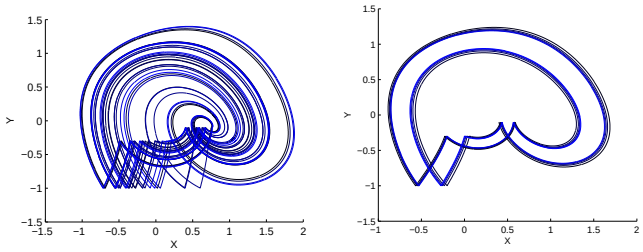

Figure 7 & 8: Chaotic behavior far from any critical value (Fig. 7) and close to a period doubling bifurcation (Fig. 8)

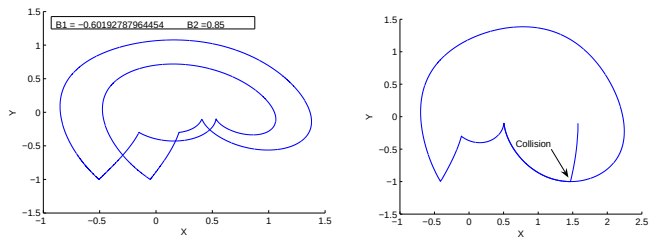

Figure 9 & 10: Fixed point at period doubling bifurcation (Fig. 9) and at collision bifurcation (Fig. 10)

Though we do not intend to address the collision bifurcations in this paper, there is no doubt it represents a major aspect of hybrid systems. In our case, it conditions the existance of numerous orbits. This means in order to make sure to obtain an exhaustive bifurcation diagram, we would have to first determine all the collision bifurcation lines and then find the fixed points for each collision-free area. For this system, we just computed one bifurcation curve (GB) by setting a Poincaré map on the point where the tangent to the solution is parallel to the switching border and iterate until that point reaches the border itself. It is also worth noticing that the change from 2 to 3 states radically changes the bifurcation diagram, although we chose switching conditions to keep phase portraits very much alike (Original Alpazur oscillator has been analysed by Ref. [1] with this method, while the model was proposed and analysed by Ref. [2] using a linear approximation).

4. Conclusion

In between other considerations, one major issue when performing such analysis is the problem of precision. Since our final target is a computer-based tool, we rely on multiple numerical methods, representing as many sources of numerical error. Our efforts are now mainly focused on the balance between precision, stability, genericity, and computation time. Eventually, the question of Collision bifurcations which are typical of hybrid systems seems to be the logical continuity of this work.

Acknowledgments

The authors would like to thank NOLTA2007 organizing committee members for their fruitful suggestions and comments. They would also like to thank the University of Tokushima (Japan) and the INSA of Toulouse (France) for their respective support.

References

[1] Kousaka, T.; Ueta, T.; Kawakami, H., “Bifurcation of switched nonlinear dynamical systems,” *IEEE Trans. Circuits and Systems II: Analog and Digital Signal Processing*, Vol. 46, No. 7, pp. 878–885, Jul. 1999.

[2] H. Kawakami and R. Lozi, “Switched Dynamical Systems – dynamical of a class of circuits with switch –,” *Proc. RIMS Conf. “Structure and Bifurcations of Dynamical Systems,” ed. by S. Ushiki, World Scientific*, pp.39–58, 1992